

Binary Quantization For LLMs Through Dynamic Grouping

Xinzhe Zheng^{1,3*}, Zhen-Qun YANG², Haoran Xie³, S. Joe Qin³, Arlene Chen⁴, Fangzhen Lin¹

¹Department of Computer Science and Engineering, The Hong Kong University of Science and Technology, Hong Kong

²Department of Computing, The Hong Kong Polytechnic University, Hong Kong

³School of Data Science, Lingnan University, Hong Kong

⁴Xiaoai Robot Inc., Shanghai, China

xzhengbj@connect.ust.hk, zq-cs.yang@polyu.edu.hk, hrxie@ln.edu.hk, president@ln.edu.hk, arlenecc@xiaoai.com, flin@cse.ust.hk

Abstract

Large Language Models (LLMs) have demonstrated remarkable performance across a wide range of Natural Language Processing (NLP) tasks, but require substantial memory and computational resources. Binary quantization, which compresses model weights from 16-bit Brain Float to 1-bit representations in $\{-1, 1\}$, offers significant reductions in storage and inference costs. However, such aggressive quantization often leads to notable performance degradation compared to more conservative 4-bit quantization methods. In this research, we propose a novel optimization objective tailored for binary quantization, along with three algorithms designed to realize it effectively. Our method enhances blocked quantization by dynamically identifying optimal unstructured submatrices through adaptive grouping strategies. Experimental results demonstrate that our approach achieves an average bit length of just 1.007 bits, while maintaining high model quality. Specifically, our quantized LLaMA 3.2 3B model attains a perplexity of 8.23, remarkably close to the original 7.81, and surpasses previous SOTA BiLLM with a perplexity of only 123.90. Furthermore, our method is competitive with SOTA 4-bit approaches such as GPTQ in both performance and efficiency. The compression process is highly efficient, requiring only 14 seconds to quantize the full LLaMA 3.2 3B weights on a single CPU core, with the entire process completing in under 100 minutes and exhibiting embarrassingly parallel properties.

Code —

https://github.com/johnnyzheng0636/WGM_bi_quan

Introduction

LLMs such as LLaMA (Dubey et al. 2024), DeepSeek (Guo et al. 2025), and Gemma (Gemma-Team et al. 2025) have demonstrated impressive performance on various NLP benchmarks, often exceeding human capabilities. These models have been improving their performance and size annually. For example, the DeepSeek R1 model has 671 billion parameters and requires at least 720GB of memory for loading, which means one NVIDIA DGX H100 can just hold

*The work was done while the author was affiliated with Department of Computer Science and Engineering, The Hong Kong University of Science and Technology

it in memory for inference. This overwhelming memory requirement limits the deployment of top LLMs and increases hosting costs. Consequently, deploying even smaller LLM versions on constrained devices like mobile phones and laptops presents significant challenges. To address this, various model compression methods have been developed, with quantization emerging as a particularly promising approach.

Quantization compresses models by sacrificing numeric precision for reduced memory requirements and faster inference speeds (Dettmers et al. 2022). This process involves mapping the original high-precision model weights to lower-precision weights, which reduce memory requirement and enable faster operations, though it may lead to a decline in model performance. There are two main types of quantization: Post Training Quantization (PTQ) and Quantization Aware Training (QAT). PTQ quantizes a pre-trained model directly into a compressed version for inference (Huang et al. 2024), while QAT necessitates training the model from scratch, enabling it to learn better quantization (Wang et al. 2023). Consequently, QAT demands computational resources comparable to training LLMs from scratch, a highly time-consuming and costly process. In contrast, PTQ quantizes LLMs within hours, rendering it particularly suitable for scenarios with limited time and computational resources.

Despite the success of 4-bit quantization (Frantar et al. 2022; Liu et al. 2025) in compressing LLMs with a negligible performance degradation, the increasing size of models demands more aggressive quantization like binary quantization. However, reducing model weights to 1 bit has not yet achieved a satisfactory performance degradation. Recent binary PTQ ,BiLLM (Huang et al. 2024), only achieved a perplexity of 35.04 with an average bit length of 1.09 for the LLaMA 7B model with an original full precision (FP) perplexity of 5.68.

To enhance existing methods, it has been observed that most research focuses on identifying the weight critical to model performance using Hessian (Huang et al. 2024; Zhao et al. 2025) and then applies non-uniform quantization based on weight importance, or accelerates this process through faster Hessian approximation or activation (Kang et al. 2025; Kim et al. 2025). Existing methodologies often exhibit a narrow reliance on uniform blocking techniques and salient

weight identification using Hessian, neglecting the exploration of alternative or adaptive grouping strategies despite their potential benefits. It is further noticed that BiLLM first segments the original matrix into a uniform grid of structured sub-matrices. Then, within each sub-matrix, elements are further divided into different unstructured sub-sub-matrices based on Hessian and magnitude distribution. Unstructured sub-matrix refers to the sub-matrix that is constructed with nonconsecutive elements in the original matrix, but from arbitrary rows and columns. This raises an important question regarding binary quantization performance: *How does the quantization performance of using unstructured sub-matrices compare to that of unstructured sub-sub-matrices within structured sub-matrices from the original weight matrix?*

In this work, we try to answer the above question. We propose a Dynamic Grouping optimization objective aimed at enhancing binary quantization efficiency. By systematically identifying optimal groupings of unstructured sub-matrices without Hessian, we provide a framework that addresses the limitations of previous quantization methods. Furthermore, we develop three algorithms designed to realize it effectively and utilize simulations to provide empirical evidence that supports these theoretical insights. The main contributions of this paper are summarized as follows.

- **Novel Optimization Framework:** We introduce a dynamic grouping optimization objective that addresses quantization loss. This approach identifies optimal groups of unstructured sub-matrices to minimize a predetermined binary quantization loss for any given matrix.
- **Three Algorithmic Solutions:** Building on our novel optimization framework, we develop three distinct algorithms:
 - 1. Dynamic Grouping:** An optimal algorithm based on classic dynamic programming;
 - 2. Greedy Grouping:** A fast, approximate algorithm of Dynamic Grouping; and
 - 3. Windowed Greedy Merging:** An even more efficient approximate algorithm of Dynamic Grouping. These algorithms are designed to balance speed and performance in various usage environments. This diversity allows for flexibility, catering to scenarios that prioritize either optimal performance or execution speed, or both.
- **Experiment results:** We conduct extensive experiments comparing our Windowed Greedy Merging-LLM, which offers the most practical trade-off for contemporary LLM architectures, with state-of-the-art (SOTA) methods. The results demonstrate that our method significantly outperforms SOTA 1-bit quantization techniques. Moreover, it achieves competitive, and in some cases even superior, performance compared to SOTA 4-bit approach, effectively balancing speed and accuracy.

Through these contributions, we advance the frontier of binary quantization for LLMs, showcasing the potential for improved model efficiency.

Related Work

Binary quantization of modern deep neural networks focused on extreme model compression through 1-bit weight and activation representations (Rastegari et al. 2016; Courbariaux, Bengio, and David 2015). Binary Connect shows it

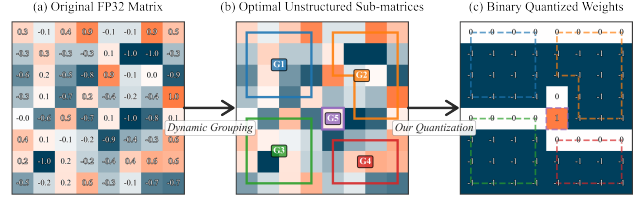


Figure 1: A basic overview of our binary quantization for LLMs through dynamic grouping.

is possible to QAT a neural network for binary weight using a straight-through estimator, and treat the weight as an identity function during backpropagation (Courbariaux, Bengio, and David 2015). Meanwhile, XNOR-Net (Rastegari et al. 2016) demonstrates the possibility of binarizing Convolutional Neural Networks (CNNs) using PTQ with an optimization objective. The optimization objective of XNOR-Net is still actively being used for the current binary quantization of LLMs:

$$\alpha^*, \mathbf{B}^* = \arg \min_{\alpha, \mathbf{B}} \|\mathbf{W} - \alpha \mathbf{B}\| \quad (1)$$

Where $\mathbf{W} \in \mathbb{R}^{m \times n}$ is the original weight to be quantized, $\mathbf{B} \in \{-1, 1\}^{m \times n}$ is the binary quantized weight, and $\alpha \in \mathbb{R}$ is the scaler of \mathbf{B} . So we can represent the original FP weight using only one 1-bit matrix plus a scaler of FP. The solution of this optimization objective is proved in XNOR-Net as:

$$\alpha^* = \frac{\|\mathbf{W}\|_1}{n}, \mathbf{B}^* = \text{sign}(\mathbf{W})$$

Where n is the total number of elements in \mathbf{W} . So α^* is the average magnitude of \mathbf{W} and \mathbf{B}^* is the element-wise direction of \mathbf{W} .

Currently, binary quantization of LLMs using QAT with a straight-through estimator can achieve performance comparable to that of FP LLMs across various NLP tasks. BitNet b1.58 2B4T (Ma et al. 2025) attained average performance of 54.19 across a wide range of benchmarks, which outperformed LLaMA 3.2 1B (44.90), Gemma-3 1B (43.74), SmoILM2 1.7B (Allal et al. 2025) (48.70), and MiniCPM 2B (Hu et al. 2024) (42.05), while only underperformed by Qwen2.5 1.5B (Yang et al. 2024) (55.23). However, binary quantization of LLMs with PTQ using modified optimization objective in XNOR-Net still has noticeable performance drop (Shang et al. 2023; Huang et al. 2024; Kim et al. 2025; Zhao et al. 2025). PB-LLM (Shang et al. 2023) use Hessian to identify salient weight and quantize those to 8-bit to minimize quantization error, remaining weight are quantized to 1 bit. BiLLM (Huang et al. 2024) modified blocked quantization from GPTQ (Frantar et al. 2022) by adding salient weight identification using Hessian and non-salient weight splitting using weight magnitude distribution. Also, the quantization loss 1 is applied once for two non-salient groups while recursively applied twice for the salient group. Finally, the quantization takes place for every salient group and two non-salient groups within each structured block. BiLLM attained perplexity of 69.97 and 49.55 on OPT 1.3B and 2.7B (Zhang et al. 2022) with FP perplexity of 14.62 and 12.47

respectively. PTQ1.61 (Zhao et al. 2025) modified BiLLM by using different salient weight strategies, where a structured salient weight is identified in the whole matrix; this approach sacrificed low bit length for better quantization model performance. Those work relies on Hessian calculation which required significant amount of computation power. AG-BiLLM (Kim et al. 2025) modified BiLLM from using Hessian to identify salient weight identification to using activation, which accelerates the quantization and reduces the memory requirement of quantization by avoiding the calculation of the Hessian matrix.

One notable observation is that, at the time of this study, all PTQ for binary quantization rely solely on simulation (Huang et al. 2024; Kim et al. 2025; Zhao et al. 2025). This is due to the lack of hardware and kernel designed for binary matrix operations, resulting in most work being based on simulated outcomes. Some of the research work in QAT, however, uses existing low-bit kernels and hardware, demonstrating that low-bit ternary LLMs can achieve significant compression and acceleration even with non-optimized hardware and kernels. For instance, BitNet2B4T (Ma et al. 2025) achieved a 12 times smaller memory size and 4.28 times inference acceleration on 2B LLMs. However, it is important to notice that BitNet2B4T quantizes each linear weight as a whole, while PTQ quantizes each linear weight either in a structured or an unstructured submatrix. So the kernel required for PTQ is different from the kernel used by BitNet2B4T, and the existing kernel and hardware are unlikely to support PTQ.

To address the above challenge of binary quantization efficiency in PTQ, in this work, we avoid the use of Hessian and focus on identifying the optimal of unstructured sub-matrices to minimize a predetermined binary quantization loss for any given matrix.

Methodology

In this section, we present the mathematical formulation for the framework of our dynamic grouping optimization, along with three algorithms designed to address the challenges of binary quantization performance in LLMs. We then discuss the determination of the boundary λ , the time complexity and the storing cost of our proposed approaches.

Novel Optimization Objective

Based on the ideas discussed above, we propose a new optimization objective that minimizes the total quantization loss across all unstructured sub-matrices by identifying their optimal grouping based on a predetermined quantization loss. The following variables define our optimization objective:

- Let $\mathbf{A} \in \mathbb{R}^{m \times n}$ be the given matrix.
- Let \mathcal{A} be the all possible set of arbitrary grouping of \mathbf{A} .
- g represents the number of non-overlapping unstructured sub-matrices, satisfying $1 \geq g \geq |\mathbf{A}|$, where $|\mathbf{A}|$ denotes the total number of non-zero elements in matrix \mathbf{A} .
- $\alpha \in \mathbb{R}$ and $\mathbf{B} \in \{-1, 1\}^{m \times n}$ are used for the binary approximation of \mathbf{A} . Each α_i and \mathbf{B}_i approximates one \mathbf{A}_i , so \mathbf{B}_i refers to the same set of matrix elements as partition \mathbf{A}_i .

Thus, we partition \mathbf{B} identically to \mathbf{A} , such that $\mathbf{A}_1 = \mathbf{B}_1, \dots, \mathbf{A}_g = \mathbf{B}_g$ and $\mathcal{A} = \mathcal{B}$ in turns of matrix index. We group matrix \mathbf{A} into g non-overlapping sub-matrices $\{\mathbf{A}_1, \mathbf{A}_2, \dots, \mathbf{A}_g\} \in \mathcal{A}$. For simplicity, we focus on non-zero elements and place any zero elements into a special group, if they exist. This special group is omitted from consideration as it has a zero loss. Additionally, \mathcal{A} encompasses all possible non-overlapping partitions using all elements of \mathbf{A} . Based on this, our proposed optimization objective is:

$$g^*, \{\mathbf{A}_1^*, \dots, \mathbf{A}_g^*\} = \arg \min_{\substack{\{\mathbf{A}_1, \dots, \mathbf{A}_g\} \in \mathcal{A} \\ \{\mathbf{B}_1, \dots, \mathbf{B}_g\} \in \mathcal{B} \\ 1 \geq g \geq |\mathbf{A}|}} \sum_{i=1}^g \|\mathbf{A}_i - \alpha_i \mathbf{B}_i\|_2^2 + \sum_{i=1}^g \frac{1}{|\mathbf{B}_i|} \quad (2)$$

The optimization objective consists of two main components. The first summation represents the quantization loss. The second summation serves as a regularization term that penalizes the inverse of the group size. We penalize the inverse of the group size because smaller groups lead to more partitions, resulting in lower efficiency due to a smaller group for each scale term α . It is important to note that the partitions need not be block-structured; each partition is simply a set of elements from \mathbf{A} . When combining all g sub-matrices, we recover the original matrix \mathbf{A} . Since $|\mathbf{A}_i| = |\mathbf{B}_i|$, the optimization objective can be rewritten to

$$g^*, \{\mathbf{A}_1^*, \dots, \mathbf{A}_g^*\} = \arg \min_{\substack{\{\mathbf{A}_1, \dots, \mathbf{A}_g\} \in \mathcal{A} \\ \{\mathbf{B}_1, \dots, \mathbf{B}_g\} \in \mathcal{B} \\ 1 \geq g \geq |\mathbf{A}|}} \sum_{i=1}^g \|\mathbf{A}_i - \alpha_i \mathbf{B}_i\|_2^2 + \sum_{i=1}^g \frac{1}{|\mathbf{A}_i|}$$

As shown in Equation (1), rewrite it as

$$\arg \min_{\alpha^*, \mathbf{B}^*} \|\mathbf{A} - \alpha \mathbf{B}\|_2^2, \quad \alpha^* = \frac{\|\mathbf{A}\|_1}{|\mathbf{A}|}, \quad \mathbf{B}^* = \text{sign}(\mathbf{A})$$

By substituting the optimal values, we can rewrite the squared 2-norm.

$$\begin{aligned} \|\mathbf{A} - \alpha \mathbf{B}\|_2^2 &= \sum_{i=1}^g \sum_{j=1}^n (a_{ij} - \alpha \cdot \text{sign}(a_{ij}))^2 \\ &= \sum_{i=1}^g \sum_{j=1}^n |a_{ij}|^2 - 2\alpha \sum_{i=1}^g \sum_{j=1}^n |a_{ij}| + \sum_{i=1}^g \sum_{j=1}^n \alpha^2 \\ &= \|\mathbf{A}\|_2^2 - 2\alpha \|\mathbf{A}\|_1 + \|\mathbf{A}\| \alpha^2 \\ &= \|\mathbf{A}\|_2^2 - \frac{\|\mathbf{A}\|_1^2}{|\mathbf{A}|} \end{aligned}$$

Consider the variance of absolute value of \mathbf{A}_i , let $\tilde{\mathbf{A}}_i$ be \mathbf{A}_i with absolute value, i.e. $\tilde{a}_{ij} = |a_{ij}|$.

$$\begin{aligned} \text{Var}(\tilde{\mathbf{A}}_i) &= E[\tilde{\mathbf{A}}_i^2] - E[\tilde{\mathbf{A}}_i]^2 \\ &= \frac{1}{|\mathbf{A}_i|} \sum_{j=1}^{|\mathbf{A}_i|} |a_{ij}|^2 - \left(\frac{1}{|\mathbf{A}_i|} \sum_{j=1}^{|\mathbf{A}_i|} |a_{ij}| \right)^2 \\ &= \frac{\|\mathbf{A}_i\|_2^2}{|\mathbf{A}_i|} - \left(\frac{\|\mathbf{A}_i\|_1}{|\mathbf{A}_i|} \right)^2 \end{aligned}$$

$$|\mathbf{A}_i| \text{Var}(\tilde{\mathbf{A}}_i) = \|\mathbf{A}_i\|_2^2 - \frac{\|\mathbf{A}_i\|_1^2}{|\mathbf{A}_i|}$$

Together, we can conclude

$$\|\mathbf{A}_i - \alpha_i^* \mathbf{B}_i^*\|_2^2 = |\mathbf{A}_i| Var(\tilde{\mathbf{A}}_i)$$

Finally, we rewrite the optimization objective 2 as

$$g^*, \{\mathbf{A}_1^*, \dots, \mathbf{A}_g^*\} = \arg \min_{\{\mathbf{A}_1, \dots, \mathbf{A}_g\} \in \mathcal{A}} \sum_{i=1}^g |\mathbf{A}_i| Var(\tilde{\mathbf{A}}_i) + \sum_{i=1}^g \frac{1}{|\mathbf{A}_i|} \quad (3)$$

Proposed Three Algorithms

To address the optimization objective, we propose three algorithms, each tailored to different scenarios and requirements. Algorithm 1. Dynamic Grouping employs classic dynamic programming to guarantee optimal solutions, while Algorithm 2. Greedy Grouping adopts a heuristic strategy to improve computational efficiency with reasonable solution quality. Algorithm 3. Windowed Greedy Merging is an efficient approximation method that achieves a strong balance between quantization performance and speed. Detailed pseudocode for Algorithms 1 and 2 is given in Appendix A due to space limitations.

1. Dynamic Grouping. This algorithm formulates the optimization problem as a dynamic programming task, systematically exploring all possible groupings to find the global optimum. Firstly, we sort all entries of \mathbf{A} in ascending order while keeping track of their original indices. Next, we observe that the partition with minimum cost (referred to as the minimum cost), as defined by Equation (3), must be a continuous sub-sequence in the sorted array. This is because only continuous sub-sequences in a sorted array guarantee minimal variance. We then break the problem into sub-problems. Suppose we aim to divide n elements into k groups with minimum cost. The optimal configuration must consist of the $k-1$ groups from the first i elements with minimum cost and the remaining $n-i$ as the last group. Formally,

$$dp[k][n] = \min_{1 \leq i < n} dp[k-1][i] + f([i : n]) \quad (4)$$

Where f is the optimization objective (3), dp is the dynamic programming table, with the total row of max group number and total column of max number of elements (both including 0). And $dp[k][n]$ refers to the minimum cost of partitioning n elements into k groups, $f([i+1 : n])$ refers to the minimum cost for the remaining elements. We prove this is correct by contradiction. Assume there is a partition of k groups for n elements with lower cost than $dp[k][n]$

$$f([0 : n]) = dp[k-1][i^*] + f([i^* : n]) < dp[k][n]$$

But $dp[k][n]$ is defined as the minimum over all possible i , including i^* . This contradicts the assumption, so $dp[k][n]$ from (4) is indeed the minimum cost.

Since we proved the sub-problem is correct, we now construct the algorithm based on Equation (4). We set the initial dp_0 as a matrix full of infinite value except the first column and row.

Then we maintain two prefix sum arrays of $\|\tilde{\mathbf{A}}\|_1$ and $\|\tilde{\mathbf{A}}\|_2^2$ for effective calculation of the optimizing objective

(3). Finally, after we complete the dp matrix, the minimum of the last column is the minimum cost to partition \mathbf{A} . We find the optimal group numbers based on the row number of the minimum value. For the sub-matrix, we use another table to record each optimal split and reconstruct the optimal group by backtracking through the table. Also, we maintain a table of absolute mean for each optimal split and use it during the backtracking to get the corresponding α of each group. The algorithm directly returns the completed dynamic programming table, optimal split table, and μ table for data analysis. The details of backtracking are omitted since it is negligible.

2. Greedy Grouping. Notice that common LLMs today have linear layer weights of at least 1024×1024 or larger. This size makes precise optimal grouping impractically slow and excessively large. To address this, we improve the Algorithm 1 by approximating the optimal grouping with a greedy algorithm. This heuristic quickly generates a feasible solution by iteratively merging groups according to a greedy criterion. We begin by sorting all non-zero entries and using a min heap to store the merging costs between each group. Initially, there are $mn - 1$ possible merges, resulting in a heap size of mn . Then we pop the candidate merge with the minimum loss and update two neighbouring candidate. We continue this pop-and-update process until only the desired number of groups remains in the heap.

3. Windowed Greedy Merging. To further improve Algorithm 1, and achieve a better efficiency-quality trade-off, we modify the initial merge cost array, and propose our Algorithm 3. Windowed Greedy Merging. Instead of starting at group mn each of size 1, we start at mn/k group, where k is the window size (group size) for each initial group. We provide a detailed description of the algorithm below.

In summary, our algorithmic framework provides both theoretical optimality (via Algorithm 1) and practical efficiency (via Algorithm 2 and 3), offering flexible solutions for a wide range of problem sizes and application scenarios. **Dynamic Grouping** identifies the optimal groupings to minimize quantization loss, setting a new benchmark for performance. **Greedy Grouping** prioritizes quantization speed, accepting suboptimal groupings to enhance efficiency in applications where speed is critical. **Windowed Greedy Merging** further prioritizes quantization speed while enabling finer groupings, which efficiently manages the trade-off between speed and performance. As the most practical solution for current hardware, it addresses the optimization objective while maintaining high execution speed and solution quality.

Interpretation and Boundary of λ

We further improve the optimization objective by adding hyperparameter λ to control the regularization term. Intuitively, when $\lambda = 0$, the objective will have group size close to the number of matrix elements, and the cost will be zero. When λ is large enough, the group size be close to 1, since the regularization occupies the majority of the cost. Also, the two norms become less comparable to inverse group size as the group size increases, so we use the average two norms

Algorithm 3: Windowed Greedy Merging

```

1: procedure WINDOWED GREEDY MERGING( $\mathbf{A} \in \mathbb{R}^{m \times n}$ ,  $g$  (group size),  $k$  (window size))
2:   sort absolute value of non-zero entry into an array
3:   initial the merge cost array  $[(i \text{ (group start)}, i + k \text{ (group end)}, cost, \mu)]$  for  $i$  in range(0,  $mn - 1$ ,  $k$ )
4:   initially the ignore array
5:   heapify the merge cost array
6:   while len(merge cost array)  $> g$  do
7:     currentMerge  $\leftarrow$  heapop
8:     if currentMerge in ignore array then
9:       remove currentMerge from ignore array
10:      continue
11:    end if
12:    push two new neighbouring merges as updates
13:    update ignore array by two old merges, invalidated by the two new merges
14:  end while
15:  return merge cost array
16: end procedure

```

to close the gap in the value of both terms. Hence, the new optimization objective is

$$\min_{g \in \mathbb{N}} \frac{1}{|\mathbf{A}|} \sum_{i=1}^g \left(|\mathbf{A}_i| Var(\tilde{\mathbf{A}}_i) + \frac{\lambda}{|\mathbf{A}_i|} \right)$$

For the algorithm update, we only need to update the cost function by adding the division by the number of non-zero entries and multiplying the regularization term by λ .

To control the grouping between the return original matrix and group the whole matrix into one group, we adjust λ . We find the upper bound and lower bound of λ , which lead to one group and max groups respectively. After finding the boundary of λ we use another hyperparameter $\tilde{\lambda} \in [0, 1]$ to control $\lambda \in [\lambda_{\min}, \lambda_{\max}]$ indirectly by sliding it between maximum and minimum. This is more intuitive, since $\tilde{\lambda}$ increases effectiveness by sacrificing accuracy as it increases from 0 to 1. Additional details on the determination of the boundary of λ can be found in Appendix B.

Time Complexity

Given the input matrix $\mathbf{A} \in \mathbb{R}^{m \times n}$, the sorting of all non-zero entries takes $O(mn \log(mn))$, prefix sum and prefix squared 2 norm takes $O(mn)$, complete the dynamic programming table takes $O((mn)^2 \cdot \text{max group number})$ since computing cost using prefix sum and prefix squared 2 norm takes $O(1)$. So **Dynamic Grouping**'s time complexity is $O((mn)^3)$, which is infeasible to run to completion. Then, **Greedy Grouping** is designed to approximate the optimal solution faster. We sort all non-zero entries and use a min heap storing the merging cost between each group, i.e. heap has size mn . Then, we update the heap until only the desired number of groups remains. This greedy merging only takes $O(mn \log(mn))$ since the sorting of non-zero entries takes $O(mn \log(mn))$, popping and updating the heap takes $O(mn \log(mn))$. For the **Windowed Greedy Merging**, it

effectively reduces the time complexity to $O(\frac{mn}{k} \log(\frac{mn}{k}))$ at the cost accuracy, since we may overlook a better merge in the initial mn/k groups of size k .

Storing Cost

Our method is similar to BiLLM omitting the salient weight. It is an improvement on Bell-shaped Distribution Splitting for Binarization of BiLLM. Additionally, we add cost for extra 16BF scaler for each group.

Experimental Results

In this section, we primarily present simulation results using our Algorithm 3. Greedy Merging-LLM (WGM-LLM), which offers the most practical trade-off for contemporary LLM architectures. These results serve to validate the effectiveness of our proposed optimization framework. Additional experimental details about our three algorithms can be found in Appendix C.

Experimental Setup

We deploy WGM-LLM within the Pytorch and Transformer framework. All binarization processes and experiments are conducted on 8 Intel(R) Xeon(R) Platinum 8480+ CPU and 1 Nvidia DGX H800 GPU. Given that WGM-LLM is an efficient PTQ framework, it eliminates the Hessian calculation, allowing for completion through a single quantization process.

Models and datasets. We facilitate our method on the LLaMA, Falcon (Falcon-LLM-Team 2024) and Gemma families. We evaluate quantization performance using seven zero-shot common sense QA tasks used in related researches (Shang et al. 2023; Huang et al. 2024), enabling direct comparability with prior research, i.e. ARC-C and ARC-E (Clark et al. 2018), BooIQ (Clark et al. 2019), HellaSwag (Zellers et al. 2019), OPQA (Mihaylov et al. 2018), PIQA (Bisk et al. 2020), WinoGrande (Sakaguchi et al. 2021). Next, we conduct experiments on perplexity (PPL) using three datasets that have also been utilized in previous research (Shang et al. 2023; Huang et al. 2024), i.e. the WikiText 2 (Merity et al. 2016), the PTB (Marcus, Santorini, and Marcinkiewicz 1993) and the C4 (Raffel et al. 2020) datasets in Appendix C.

Baseline. We conduct experiments on three related quantization methods to compare them with full precision (FP) and our WGM-LLM. The primary baselines are BiLLM and PB-LLM, which represent state-of-the-art (SOTA) models for binary post-training quantization (PTQ). We also perform experiments with GPTQ, the SOTA for 4-bit PTQ, further demonstrating the efficacy of WGM-LLM under extreme binarization. AG-BiLLM is excluded due to unavailability of the source code. PTQ-1.61 is similarly omitted because its implementation lacks support for contemporary LLM architectures, and the comprehensive updates required prohibitive development effort beyond the scope of this study.

Results

Performance and speed comparison. Our experimental results demonstrate that our proposed method significantly

Model	Method	Bits	ARC-C	ARC-E	BoolQ	Hellaswag	OPQA	PIQA	Winogrande	Avg.
Llama 3.2 1B	FP	16	(0.364±0.01)	0.605±0.01	0.639±0.01	0.636±0.01	0.374±0.02	0.744±0.01	0.612±0.01	0.568
	GPTQ	4	0.335±0.01	0.561±0.01	0.577±0.01	(0.452±0.01)	(0.370±0.02)	0.726±0.01	(0.609±0.01)	0.519
	BiLLM	1.08	0.250±0.01	0.279±0.01	0.494±0.01	0.270±0.00	0.254±0.02	0.534±0.01	0.514±0.01	0.371
	PB-LLM	1.7	0.227±0.01	0.296±0.01	0.619±0.01	0.281±0.01	0.256±0.02	0.550±0.01	0.520±0.01	0.393
	WGM	1.007	0.369±0.01	(0.596±0.01)	(0.636±0.01)	0.636±0.01	0.366±0.02	(0.732±0.01)	0.590±0.01	(0.561)
Llama 3.2 3B	FP	16	0.458±0.02	0.716±0.01	0.728±0.01	0.736±0.00	0.432±0.02	0.775±0.01	0.693±0.01	0.648
	GPTQ	4	(0.444±0.02)	0.694±0.01	(0.708±0.01)	(0.722±0.01)	(0.426±0.02)	0.763±0.01	0.677±0.01	(0.633)
	BiLLM	1.08	0.224±0.01	0.325±0.01	0.617±0.01	0.319±0.01	0.252±0.02	0.557±0.01	0.508±0.01	0.400
	PB-LLM	1.7	0.213±0.01	0.309±0.01	0.624±0.01	0.294±0.01	0.266±0.02	0.556±0.01	0.494±0.01	0.394
	WGM	1.007	(0.444±0.02)	(0.695±0.01)	0.667±0.01	0.720±0.01	0.408±0.02	(0.770±0.01)	(0.685±0.01)	0.627
Falcon3-1B-Instruct	FP	16	0.453±0.02	0.680±0.01	0.732±0.01	0.631±0.01	0.404±0.02	0.750±0.01	0.601±0.01	0.607
	GPTQ	4	(0.442±0.02)	(0.678±0.01)	(0.731±0.01)	(0.626±0.01)	0.396±0.02	(0.747±0.01)	0.594±0.01	(0.602)
	BiLLM	1.08	0.236±0.01	0.415±0.01	0.596±0.01	0.363±0.01	0.300±0.02	0.613±0.01	0.527±0.01	0.436
	PB-LLM	1.7	0.233±0.01	0.354±0.01	0.622±0.01	0.331±0.01	0.270±0.02	0.595±0.01	0.505±0.01	0.416
	WGM	1.007	0.424±0.01	0.660±0.01	0.699±0.01	0.614±0.01	(0.402±0.02)	0.745±0.01	(0.598±0.01)	0.592
Falcon3-3B-Instruct	FP	16	0.544±0.02	0.749±0.01	0.788±0.01	0.701±0.01	(0.422±0.02)	(0.759±0.01)	0.649±0.01	0.659
	GPTQ	4	0.506±0.02	0.716±0.01	(0.775±0.01)	0.680±0.01	0.406±0.02	0.754±0.01	(0.648±0.01)	0.641
	BiLLM	1.08	0.224±0.01	0.310±0.01	0.496±0.01	0.307±0.01	0.246±0.02	0.559±0.01	0.534±0.01	0.382
	PB-LLM	1.7	0.206±0.01	0.316±0.01	0.623±0.01	0.307±0.01	0.256±0.02	0.575±0.01	0.513±0.01	0.399
	WGM	1.007	(0.520±0.02)	(0.740±0.01)	0.745±0.01	(0.696±0.01)	0.426±0.02	0.760±0.01	0.635±0.01	(0.646)
Gemma-3-1b-it	FP	16	0.385±0.01	(0.637±0.01)	0.759±0.01	0.578±0.01	(0.384±0.02)	(0.724±0.01)	0.589±0.01	0.579
	GPTQ	4	(0.395±0.01)	0.639±0.01	0.739±0.01	(0.555±0.01)	0.402±0.02	0.717±0.01	(0.588±0.01)	(0.576)
	BiLLM	1.08	0.232±0.01	0.296±0.01	0.423±0.01	0.272±0.00	0.266±0.02	0.523±0.01	0.493±0.01	0.358
	PB-LLM	1.7	0.233±0.01	0.303±0.01	0.466±0.01	0.281±0.01	0.270±0.02	0.540±0.01	0.514±0.01	0.372
	WGM	1.007	0.407±0.01	0.628±0.01	(0.749±0.01)	0.578±0.01	0.378±0.02	0.730±0.01	0.583±0.01	0.579
Gemma-3-4b-it	FP	16	0.571±0.02	0.779±0.01	0.839±0.01	0.744±0.00	(0.468±0.02)	0.774±0.01	0.695±0.01	0.696
	GPTQ	4	0.538±0.02	0.764±0.01	0.827±0.01	(0.727±0.00)	0.446±0.02	0.769±0.01	0.669±0.01	0.677
	BiLLM	1.08	0.236±0.01	0.367±0.01	0.621±0.01	0.347±0.01	0.280±0.02	0.586±0.01	0.450±0.01	0.420
	PB-LLM	1.7	0.247±0.01	0.345±0.01	0.590±0.01	0.327±0.01	0.274±0.02	0.547±0.01	0.497±0.01	0.404
	WGM	1.007	(0.565±0.02)	(0.778±0.01)	(0.835±0.01)	0.744±0.00	0.476±0.02	(0.773±0.01)	(0.691±0.01)	(0.695)

Table 1: Comparison of LLM performance across seven QA tasks. WGM: Windowed Greedy Merging algorithm with window size $w = 64$, and maximum group size $g = 32$. Optimal results are in bold; suboptimal results are indicated by parentheses.

Model	GPTQ	BiLLM	PB-LLM	WGM
Llama 3.2 1B	372.9	365.8	150.1	1018.4(141.0)
Llama 3.2 3B	780.4	811.8	260.4	3555.6(417.3)
Falcon3 1B Instruct	428.4	687.8	151.9	1377.4(297.5)
Falcon3 3B Instruct	772.5	720.1	263.1	2974.5(557.0)
Gemma 3 1B it	399.0	385.0	151.8	777.5(125.7)
Gemma 3 4B it	1000.8	946.7	364.8	3633.9(431.1)

Table 2: Comparison of quantization time (in Seconds). Our method using 8 CPUs vs. others using 1 GPU. The time in parentheses for WGM-LLM reflects parallel overhead.

outperforms the current SOTA quantization in several key aspects. From Table 1, we observe a significant performance improvement across all seven QA tasks and in all six models when compared to existing binary quantization methods like BiLLM and PB-LLM. Additionally, our method demonstrates competitive QA performance compared to the 4-bit quantization method, GPTQ. What’s more, its average performance across the seven QA tasks outperforms GPTQ in 4 out of the 6 models: Llama 3.2 1B, Falcon3-3B-Instruct, Gemma-3-1b-it, and Gemma-3-4b-it. From Table 2, we note that the quantization process is completed using only CPU resources in under one hour, highlighting its efficiency. Furthermore, considering the cost-effectiveness of CPUs relative

w	Bit	Time	Wikitext 2	PTB	C4	Avg.
8	1.0015	7606.56 (139.23)	9.90	17.83	14.22	13.99
16	1.0015	3753.57 (147.63)	9.90	17.91	14.24	14.02
32	1.0015	1900.39 (134.34)	9.90	17.98	14.24	14.04
64	1.0015	971.81 (133.88)	9.92	17.83	14.24	14.00
128	1.0015	571.83 (130.67)	10.11	18.08	14.59	14.26
256	1.0015	393.64 (145.25)	10.62	19.36	15.37	15.11
512	1.0015	296.62 (130.72)	12.42	27.90	18.25	19.52

Table 3: Performance comparison for selecting window size w , using Llama3.2 1B to analyze perplexity across varying w values, with $w = 256$ for efficient experimentation.

to GPUs, and assuming that the available CPUs are at least equal to the number of linear layers in LLMs, our method can theoretically achieve approximately 14 seconds of computation for parallel quantization. These results underscore the advantages of our approach in both performance and speed.

Approximation algorithm performance. Since only Algorithm 2, Greedy Grouping and Algorithm 3, Windowed Greedy Merging are feasible for actual implementation, due to Algorithm 1, Dynamic Grouping being too slow and impractical, experiments have been conducted to show how accurate can Algorithm 2 and 3 approximate the optimal solution from Algorithm 1 on a single CPU. The experi-

g	Bit	Time	Wikitext 2	PTB	C4	Avg.
8	1.000	429.50(177.39)	7677	5165	4819	5887
16	1.000	374.81(128.15)	12.61	24.05	18.51	55.17
32	1.000	371.82 (127.25)	10.94	20.21	15.92	15.69
64	1.000	428.05(174.66)	10.65	19.45	15.45	15.19
128	1.000	385.05(135.06)	10.62	19.37	15.39	15.13
256	1.002	393.64(145.25)	10.62	19.36	15.37	15.11
512	1.003	383.77(145.77)	10.62	19.35	15.36	15.11
1629038	4	4642.47(67.84)	9.92	17.88	14.30	14.03

Table 4: Performance comparison for selecting “maximum group size” g . Utilizing Llama3.2 1B to analyze Perplexity across varying g values with $w=256$ for efficient experimentation. In the final row, the group size increases until the bit length reaches 4, indicating algorithm generalizability; here, the window is set to 4, and g represents the average group.

λ	Time	Wikitext 2	PTB	C4	Avg.
0.0	340.10 (111.23)	10.60	19.24	15.34	15.06
0.1	391.23 (132.98)	10.61	19.29	15.37	15.09
0.2	385.21 (133.20)	10.61	19.29	15.36	15.09
0.3	394.20 (134.01)	10.61	19.27	15.36	15.08
0.4	377.17 (130.04)	10.61	19.29	15.38	15.09
0.5	386.47 (129.55)	10.61	19.28	15.37	15.09
0.6	370.80 (126.68)	10.62	19.32	15.39	15.11
0.7	378.87 (127.96)	10.62	19.35	15.38	15.11
0.8	364.53 (130.19)	10.62	19.34	15.36	15.10
0.9	374.72 (133.59)	10.62	19.34	15.39	15.12
1.0	364.32 (129.50)	10.61	19.32	15.37	15.10

Table 5: Performance comparison for selecting λ . Utilizing Llama3.2 1B to analyze Perplexity across varying λ values with $w=256$ and $g=256$ for efficient experimentation.

ments used a randomly generated normally distributed matrix of $\mu = 0, \sigma = 1$ to simulate a full LLM weight. Firstly, all three algorithms have their quantization loss in terms of Mean Square Error (MSE) and quantization speed test on a small squared matrix. As shown in Appendix C, the MSE of all three proposed algorithms are nearly 0 while having insignificant difference and are overlapping in the graph. This indicates that Algorithms 2 and 3 can accurately approximate the optimal solution of Algorithm 1. As the size of the matrix increase, Algorithm 1 become impractical. To save computational resources and time, experiments for the biggest matrix were conducted solely with Algorithm 2 and 3. As expected, the MSE loss of both approximation algorithms for bigger matrix (from 2 to 2048 squared matrices, increasing by powers of 2) are again nearly 0 while having insignificant difference and are overlapping in the graph. This suggests that both approximation algorithms can accurately approximate the optimal solution. Additionally, the actual speeds of Algorithms 2 and 3 are also tested in Appendix C. The results show Algorithm 3, Windowed Greedy Merging can quantize a squared matrix of size 2048 under 10 seconds, while Algorithm 2 requires more than 1000 seconds. Since modern LLMs generally use square matrices of approximately size 2048, we can conclude that Algorithm 3 can quantize modern LLMs in a reasonable amount of time. Conversely, Algorithm 2 is practical but requires three orders

of magnitude more time to solve the same optimization problem. Therefore, only Algorithm 3 can accurately achieve the optimization objective within a reasonable time cost.

Hyperparameters. Regarding the hyperparameters, we conducted relevant experiments to assess how hyperparameter variations affect performance and to select the optimal hyperparameters. Our results provide valuable insights into the hyperparameter variations affecting performance. The analysis of **window size** w in Table 3 reveals that perplexity begins to decrease significantly when w exceeds 64, leading us to choose $w = 64$ for an optimal balance between perplexity and quantization time. Similarly, Table 4 shows that the **maximum group size** g achieves flat performance improvements at $g = 32$, prompting us to adopt this value for shorter bit lengths while maintaining good performance. Lastly, the variation of **regularization term** λ demonstrates a negligible impact on quantization performance, as indicated in Table 5. We use $\lambda = 0.75$ based on the experiments and boundary of λ in Appendix B.

Conclusion, Limitations and Future Work

This work introduces a new optimization objective and three tailored algorithms to address the binary quantization challenge in LLMs by identifying the optimal unstructured sub-matrix partition that minimizes the proposed optimization objective. We demonstrate the effectiveness of our approach on three datasets and various evaluation criteria. The Algorithm 3, WGM-LLM significantly outperforms SOTA binary quantization in QA tasks and perplexity, achieving an average bit length of just 1.007 bits, significantly lower than current SOTA averages. Moreover, it is competitive with SOTA 4-bit quantization method, GPTQ, and even outperforms GPTQ on most QA tasks. What’s more, it balances performance and speed in the trade-off effectively. It can achieve approximately 14 seconds of computation for parallel quantization, theoretically, given adequate CPU. This research pushes the boundaries of binary quantization in LLMs, highlighting the potential for deployment on constrained devices and encouraging further exploration in this area.

Limitations and future work: Currently, there is no hardware designed for 1-bit operations, limiting our quantization to simulation. Additionally, existing kernels are not optimized for our algorithm. Unlike structured block partitioning that utilizes CUDA kernels, our arbitrary partitioning lacks such optimization. This results in two key limitations: First, traditional methods easily achieve average bit length using a single scaler, while our approach requires additional bits to store indices of the unstructured matrix. Second, the lack of optimized kernels leads to suboptimal inference speeds. Therefore, our study is currently limited to simulations; actual bit width and latency will depend on future hardware support.

To accelerate the algorithm, we can use C++ instead of Python, additionally PyTorch supports C++, allowing for further parallelization. We can also improve the algorithm by finding faster alternatives to WGM-LLM that enhance quantized LLM performance. Additionally, exploring better optimization objectives for binary quantization is also

promising research direction. Finally, developing kernels and hardware tailored for binary LLMs is crucial for maximizing their potential. Adapting existing kernels to implement our quantization methods on current hardware will help us evaluate the achievable size reduction and acceleration. Lastly, as a side note, with 16 groups, the algorithm can fit into exist 4-bit kernel and hardware, with minimal performance degradation compared to GPTQ, establishing a viable new approach for 4-bit quantization research.

References

Allal, L. B.; Lozhkov, A.; Bakouch, E.; Blázquez, G. M.; Penedo, G.; Tunstall, L.; Marafioti, A.; Kydlícek, H.; Lajarín, A. P.; Srivastav, V.; et al. 2025. SmoILM2: When Smo Goes Big-Data-Centric Training of a Small Language Model. *CoRR*.

Bisk, Y.; Zellers, R.; Le bras, R.; Gao, J.; and Choi, Y. 2020. PIQA: Reasoning about Physical Commonsense in Natural Language. *Proceedings of the AAAI Conference on Artificial Intelligence*, 34(05): 7432–7439.

Clark, C.; Lee, K.; Chang, M.-W.; Kwiatkowski, T.; Collins, M.; and Toutanova, K. 2019. BoolQ: Exploring the Surprising Difficulty of Natural Yes/No Questions. In Burstein, J.; Doran, C.; and Solorio, T., eds., *Proceedings of the 2019 Conference of the North American Chapter of the Association for Computational Linguistics: Human Language Technologies, Volume 1 (Long and Short Papers)*, 2924–2936. Minneapolis, Minnesota: Association for Computational Linguistics.

Clark, P.; Cowhey, I.; Etzioni, O.; Khot, T.; Sabharwal, A.; Schoenick, C.; and Tafjord, O. 2018. Think you have Solved Question Answering? Try ARC, the AI2 Reasoning Challenge. arXiv:1803.05457.

Courbariaux, M.; Bengio, Y.; and David, J.-P. 2015. BinaryConnect: training deep neural networks with binary weights during propagations. In *Proceedings of the 29th International Conference on Neural Information Processing Systems - Volume 2*, 3123–3131. Cambridge, MA, USA: MIT Press.

Dettmers, T.; Lewis, M.; Belkada, Y.; and Zettlemoyer, L. 2022. LLM.int8(): 8-bit Matrix Multiplication for Transformers at Scale. arXiv:2208.07339.

Dubey, A.; Jauhri, A.; Pandey, A.; Kadian, A.; Al-Dahle, A.; Letman, A.; Mathur, A.; Schelten, A.; Yang, A.; Fan, A.; et al. 2024. The Llama 3 Herd of Models. arXiv:2407.21783.

Falcon-LLM-Team. 2024. The Falcon 3 Family of Open Models.

Frantar, E.; Ashkboos, S.; Hoefler, T.; and Alistarh, D. 2022. GPTQ: Accurate Post-training Compression for Generative Pretrained Transformers. arXiv:2210.17323.

Gemma-Team, G.; Kamath, A.; Ferret, J.; Pathak, S.; Vieillard, N.; Merhej, R.; Perrin, S.; Matejovicova, T.; Ramé, A.; Rivière, M.; et al. 2025. Gemma 3 technical report. *arXiv preprint arXiv:2503.19786*.

Guo, D.; Yang, D.; Zhang, H.; Song, J.; Zhang, R.; Xu, R.; Zhu, Q.; Ma, S.; Wang, P.; Bi, X.; et al. 2025. DeepSeek-R1: Incentivizing Reasoning Capability in LLMs via Reinforcement Learning. arXiv:2501.12948.

Hu, S.; Tu, Y.; Han, X.; He, C.; Cui, G.; Long, X.; Zheng, Z.; Fang, Y.; Huang, Y.; Zhao, W.; et al. 2024. MiniCPM: Unveiling the Potential of Small Language Models with Scalable Training Strategies. *CoRR*.

Huang, W.; Liu, Y.; Qin, H.; Li, Y.; Zhang, S.; Liu, X.; Magno, M.; and Qi, X. 2024. BiLLM: pushing the limit of post-training quantization for LLMs. In *Proceedings of the 41st International Conference on Machine Learning*, 20023–20042.

Kang, Y.; Luo, Z.; Wen, M.; Shi, Y.; He, J.; Yang, J.; Xue, Z.; Feng, J.; and Liu, X. 2025. HWPQ: Hessian-free Weight Pruning-Quantization For LLM Compression And Acceleration. arXiv:2501.16376.

Kim, A.; Lee, E.; Lee, M.; Kim, Y.; and Jang, S.-J. 2025. AG-BiLLM: Activation-Guided Fully Binarized Large Language Models. In *2025 International Conference on Electronics, Information, and Communication (ICEIC)*, 1–4. IEEE.

Liu, Z.; Zhao, C.; Fedorov, I.; Soran, B.; Choudhary, D.; Krishnamoorthi, R.; Chandra, V.; Tian, Y.; and Blankevoort, T. 2025. SpinQuant: LLM Quantization with Learned Rotations. In *The Thirteenth International Conference on Learning Representations*.

Ma, S.; Wang, H.; Huang, S.; Zhang, X.; Hu, Y.; Song, T.; Xia, Y.; and Wei, F. 2025. BitNet b1.58 2B4T Technical Report. arXiv:2504.12285.

Marcus, M. P.; Santorini, B.; and Marcinkiewicz, M. A. 1993. Building a Large Annotated Corpus of English: The Penn Treebank. *Computational Linguistics*, 19(2): 313–330.

Merity, S.; Xiong, C.; Bradbury, J.; and Socher, R. 2016. Pointer Sentinel Mixture Models. arXiv:1609.07843.

Mihaylov, T.; Clark, P.; Khot, T.; and Sabharwal, A. 2018. Can a Suit of Armor Conduct Electricity? A New Dataset for Open Book Question Answering. In Riloff, E.; Chiang, D.; Hockenmaier, J.; and Tsujii, J., eds., *Proceedings of the 2018 Conference on Empirical Methods in Natural Language Processing*, 2381–2391. Brussels, Belgium: Association for Computational Linguistics.

Raffel, C.; Shazeer, N.; Roberts, A.; Lee, K.; Narang, S.; Matena, M.; Zhou, Y.; Li, W.; and Liu, P. J. 2020. Exploring the Limits of Transfer Learning with a Unified Text-to-Text Transformer. *Journal of Machine Learning Research*, 21(140): 1–67.

Rastegari, M.; Ordonez, V.; Redmon, J.; and Farhadi, A. 2016. XNOR-Net: ImageNet Classification Using Binary Convolutional Neural Networks. In *Computer Vision – ECCV 2016*, 525–542. Cham: Springer International Publishing.

Sakaguchi, K.; Bras, R. L.; Bhagavatula, C.; and Choi, Y. 2021. WinoGrande: an adversarial winograd schema challenge at scale. *Commun. ACM*, 64(9): 99–106.

Shang, Y.; Yuan, Z.; Wu, Q.; and Dong, Z. 2023. Pb-llm: Partially binarized large language models. arXiv:2310.00034.

Wang, H.; Ma, S.; Dong, L.; Huang, S.; Wang, H.; Ma, L.; Yang, F.; Wang, R.; Wu, Y.; and Wei, F. 2023. BitNet: Scaling 1-bit Transformers for Large Language Models. arXiv:2310.11453.

Yang, A.; Yang, B.; Zhang, B.; Hui, B.; Zheng, B.; Yu, B.; Li, C.; Liu, D.; Huang, F.; Wei, H.; et al. 2024. Qwen2. 5 Technical Report. *CoRR*.

Zellers, R.; Holtzman, A.; Bisk, Y.; Farhadi, A.; and Choi, Y. 2019. HellaSwag: Can a Machine Really Finish Your Sentence? In Korhonen, A.; Traum, D.; and Márquez, L., eds., *Proceedings of the 57th Annual Meeting of the Association for Computational Linguistics*, 4791–4800. Florence, Italy: Association for Computational Linguistics.

Zhang, S.; Roller, S.; Goyal, N.; Artetxe, M.; Chen, M.; Chen, S.; Dewan, C.; Diab, M.; Li, X.; Lin, X. V.; Mihaylov, T.; Ott, M.; Shleifer, S.; Shuster, K.; Simig, D.; Koura, P. S.; Sridhar, A.; Wang, T.; and Zettlemoyer, L. 2022. OPT: Open Pre-trained Transformer Language Models. arXiv:2205.01068.

Zhao, J.; Zhang, M.; Wang, M.; Shang, Y.; Zhang, K.; Guan, W.; Wang, Y.; and Zhang, M. 2025. PTQ1.61: Push the Real Limit of Extremely Low-Bit Post-Training Quantization Methods for Large Language Models. arXiv:2502.13179.

Appendix A: Our Three Algorithms

In this section, we present pseudocode of our designed algorithms:

- Algorithms 1: Dynamic Grouping.
- Algorithms 2: Greedy Grouping.

Algorithm 2: Greedy Grouping

```

procedure GREEDY MERGING( $A \in \mathbb{R}^{m \times n}$ ,  

 $g$  (group size))  

2:   sort absolute value of non-zero entry into an array  

   initial the merge cost array  $[(i \text{ (group start)}, i +$   

 $1 \text{ (group end)}, cost, \mu)]$  for  $i$  in range( $mn - 1$ )  

4:   initially the ignore array  

   heapify the merge cost array  

6:   while len(merge cost array)  $> g$  do  

     currentMerge  $\leftarrow$  heapop  

8:     if currentMerge in ignore array then  

       remove currentMerge from ignore array  

       continue  

end if  

12:    push two new merges as updates  

       update ignore array by two merged, invalidated  

       by the two new merges  

14:   end while  

   return merge cost array  

16: end procedure

```

Algorithm 1: Dynamic Grouping

```

1: procedure SORT( $A$ )  

2:   sort the absolute value of input matrix  $A$   

3:   return Sorted array of value and index in  $A$   

4: end procedure  

5: procedure PREFIX SUM(Array)  

6:   prefix_sum, squared_prefix_sum  $\leftarrow$  empty array  

7:   for  $i$  in Array do  

8:     prefix_sum  $\leftarrow$  [prefix_sum,  $i$ ]  

9:     squared_prefix_sum  $\leftarrow$  [squared_prefix_sum,  $i^2$ ]  

10:  end for  

11:  return prefix_sum, squared_prefix_sum  

12: end procedure  

13: procedure COST( $j, k$ , prefix_sum, squared_prefix_sum)  

14:   group_size  $\leftarrow k - j$   

15:   abs_sum  $\leftarrow$  prefix_sum[ $k$ ] - prefix_sum[ $j$ ]  

16:   abs_sum_sqr  $\leftarrow$  squared_prefix_sum[ $k$ ] -  

     squared_prefix_sum[ $j$ ]  

17:    $\mu \leftarrow \frac{abs\_sum}{group\_size}$   

18:    $\sigma^2 \leftarrow \frac{abs\_sum\_sqr}{group\_size} - \mu^2$   

19:   cost  $\leftarrow group\_size\sigma^2 + \frac{1}{group\_size}$   

20:   return cost,  $\mu$   

21: end procedure  

22: procedure DYNAMIC GROUPING( $A \in \mathbb{R}^{m \times n}$ )  

23:    $dp \leftarrow dp_0, j^* \leftarrow \emptyset \in \mathbb{R}^{m \times n}$   

24:    $a, i \leftarrow$  SORT( $A$ )  

25:    $p_1, p_2 \leftarrow$  PREFIX SUM( $a$ )  

26:   for  $i$  in 1 to  $mn$  do  

27:     for  $j$  in 1 to  $mn$  do  

28:        $c_{min} = \inf, j^* = -1, \mu^* = -1$   

29:       for  $k$  in 0 to  $j - 1$  do  

30:         if  $k$  in  $j^*[:i][k - 1]$  then  

           continue  

end if  

32:          $c, \mu \leftarrow$  COST( $k, j, p_1, p_2$ )  

33:          $c \leftarrow c + dp[i - 1][k]$   

34:         if  $c < c_{min}$  then  

35:            $c_{min} \leftarrow c, j^* = j, \mu^* = \mu$   

36:         end if  

37:       end for  

38:        $dp[i][j] \leftarrow c_{min}, j^*[i][j] \leftarrow j^*, \mu[i][j] \leftarrow \mu^*$   

39:     end for  

40:   end for  

41:   return  $dp, j^*, \mu$   

43: end procedure

```

Appendix B: Determining the Boundary of λ

Firstly, we determine the lower bound of λ . Considering the case of group size 1 and number of group g is the number of non-zero elements n . The cost is

$$\sum_{i=1}^g 0 + \lambda \frac{1}{1} = n\lambda \quad (5)$$

The squared 2 norm is 0 since in the case of group size one $A_i = \alpha_i B_i$.

Now consider the case of the number of groups = $g - 1$, so we have $g - 2$ groups of size 1 and 1 group of size 2. The cost is

$$\sum_{i=1}^{g-2} \left(0 + \lambda \frac{1}{1} \right) + \frac{1}{n} (|a_1| - \alpha^*)^2 + \frac{1}{n} (|a_2| - \alpha^*)^2 + \frac{\lambda}{2}$$

$$\begin{aligned}
&= \sum_{i=1}^{n-2} \left(0 + \lambda \frac{1}{1} \right) + \frac{1}{n} (|a_1| - \frac{|a_1| + |a_2|}{2})^2 \\
&\quad + \frac{1}{n} (|a_2| - \frac{|a_1| + |a_2|}{2})^2 + \frac{\lambda}{2} \\
&= (n-2)\lambda + \frac{1}{n} (\frac{|a_1| - |a_2|}{2})^2 + \frac{1}{n} (\frac{|a_2| - |a_1|}{2})^2 + \frac{\lambda}{2} \\
&= (n-2)\lambda + \frac{1}{n} (\frac{|a_1| - |a_2|}{2})^2 + \frac{1}{n} (\frac{|a_1| - |a_2|}{2})^2 + \frac{\lambda}{2} \\
&= (n-2)\lambda + \frac{(|a_1| - |a_2|)^2}{2n} + \frac{\lambda}{2}
\end{aligned} \tag{6}$$

Since we are minimizing the objective, when (5) < (6) we have n groups, else at most n-1 groups. Because we are using quantization for higher efficiency, a smaller group with a bigger size is desired, so we must avoid the n group case, such as we want (5) > (6).

$$\begin{aligned}
n\lambda &> (n-2)\lambda + \frac{(|a_1| - |a_2|)^2}{2n} + \frac{\lambda}{2} \\
2\lambda &> \frac{(|a_1| - |a_2|)^2}{2n} + \frac{\lambda}{2} \\
\frac{3\lambda}{2} &> \frac{(|a_1| - |a_2|)^2}{2n} \\
\lambda &> \frac{(|a_1| - |a_2|)^2}{3n} \\
\lambda &> \min_{1 \leq i < n} \frac{(|a_i| - |a_{i+1}|)^2}{3n}
\end{aligned}$$

Since we want to avoid the n-1 group case too, and in general any group number leading to a small group size. So a good λ will not be in the close neighbourhood of the actual lower bound, thus we can estimate the lower bound with a rough number

$$\lambda > \frac{(|a_1| - |a_2|)^2}{3n} > \min_{1 \leq i < n} \frac{(|a_i| - |a_{i+1}|)^2}{3n}$$

We can just use the first two elements in the sorted array for fast computation and estimation of the lower bound of λ , so we have a lower bound

$$\lambda > \frac{(|a_1| - |a_2|)^2}{3n} \tag{7}$$

Next, we deduce the upper bound for λ with a similar method. Considering the case of one group, the cost is

$$\begin{aligned}
&\frac{1}{|\mathbf{A}|} |\mathbf{A}| Var(\tilde{\mathbf{A}}) + \frac{\lambda}{|\mathbf{A}|} \\
&= \frac{1}{n} n Var(\tilde{\mathbf{A}}) + \frac{\lambda}{n} \\
&= Var(\tilde{\mathbf{A}}) + \frac{\lambda}{n}
\end{aligned} \tag{8}$$

Considering two group of matrix $\mathbf{A}_1, \mathbf{A}_2$ split at k^{th} sorted non-zero element of \mathbf{A} , the cost is

$$\begin{aligned}
&\frac{1}{|\mathbf{A}|} |\mathbf{A}_1| Var(\tilde{\mathbf{A}}_1) + \frac{\lambda}{|\mathbf{A}_1|} + \frac{1}{|\mathbf{A}|} |\mathbf{A}_2| Var(\tilde{\mathbf{A}}_2) + \frac{\lambda}{|\mathbf{A}_2|} \\
&= \frac{1}{n} \left(k Var(\tilde{\mathbf{A}}_1) + (n-k) Var(\tilde{\mathbf{A}}_2) \right) + \frac{\lambda}{k} + \frac{\lambda}{n-k}
\end{aligned} \tag{9}$$

If we want to have at least 2 group, (9) < (8),

$$\begin{aligned}
&\frac{1}{n} \left(k Var(\tilde{\mathbf{A}}_1) + (n-k) Var(\tilde{\mathbf{A}}_2) \right) + \frac{\lambda}{k} + \frac{\lambda}{n-k} < Var(\tilde{\mathbf{A}}) + \frac{\lambda}{n} \\
&k Var(\tilde{\mathbf{A}}_1) + (n-k) Var(\tilde{\mathbf{A}}_2) + \frac{n\lambda}{k} + \frac{n\lambda}{n-k} < n Var(\tilde{\mathbf{A}}) + \lambda \\
&\frac{n\lambda}{k} + \frac{n\lambda}{n-k} - \lambda < n Var(\tilde{\mathbf{A}}) - \left(k Var(\tilde{\mathbf{A}}_1) + (n-k) Var(\tilde{\mathbf{A}}_2) \right) \\
&\lambda \left(\frac{n}{k} + \frac{n}{n-k} - 1 \right) < n Var(\tilde{\mathbf{A}}) - \left(k Var(\tilde{\mathbf{A}}_1) + (n-k) Var(\tilde{\mathbf{A}}_2) \right) \\
&\lambda < \frac{n Var(\tilde{\mathbf{A}}) - \left(k Var(\tilde{\mathbf{A}}_1) + (n-k) Var(\tilde{\mathbf{A}}_2) \right)}{\frac{n}{k} + \frac{n}{n-k} - 1}
\end{aligned}$$

Notice we can simplify the above expression by rewriting $n Var(\tilde{\mathbf{A}})$

$$n Var(\tilde{\mathbf{A}}) = \sum_{x \in \tilde{\mathbf{A}}} (x - \mu)^2 = \sum_{x_1 \in \tilde{\mathbf{A}}_1} (x_1 - \mu)^2 + \sum_{x_2 \in \tilde{\mathbf{A}}_2} (x_2 - \mu)^2$$

Where μ is the average of elements of $\tilde{\mathbf{A}}$. Notice

$$\begin{aligned}
\sum_{x_1 \in \tilde{\mathbf{A}}_1} (x_1 - \mu)^2 &= \sum_{x_1 \in \tilde{\mathbf{A}}_1} ((x_1 - \mu_1) + (\mu_1 - \mu))^2 \\
&= \sum_{x_1 \in \tilde{\mathbf{A}}_1} (x_1 - \mu_1)^2 + 2(x_1 - \mu_1)(\mu_1 - \mu) + (\mu_1 - \mu)^2 \\
&= \left(\sum_{x_1 \in \tilde{\mathbf{A}}_1} ((x_1 - \mu_1)^2 + (\mu_1 - \mu)^2) \right) + \\
&\quad \left(2(\mu_1 - \mu) \sum_{x_1 \in \tilde{\mathbf{A}}_1} (x_1 - \mu_1) \right) \\
&= \left(\sum_{x_1 \in \tilde{\mathbf{A}}_1} ((x_1 - \mu_1)^2 + (\mu_1 - \mu)^2) \right) + \\
&\quad \left(2(\mu_1 - \mu) \left(\left(\sum_{x_1 \in \tilde{\mathbf{A}}_1} x_1 \right) - |\tilde{\mathbf{A}}_1| \mu_1 \right) \right) \\
&= \left(\sum_{x_1 \in \tilde{\mathbf{A}}_1} ((x_1 - \mu_1)^2 + (\mu_1 - \mu)^2) \right) + (2(\mu_1 - \mu)(0)) \\
&= \left(\sum_{x_1 \in \tilde{\mathbf{A}}_1} ((x_1 - \mu_1)^2 + (\mu_1 - \mu)^2) \right) \\
&= \sum_{x_1 \in \tilde{\mathbf{A}}_1} (x_1 - \mu_1)^2 + k(\mu_1 - \mu)^2
\end{aligned}$$

Similarly

$$\begin{aligned}
\sum_{x_2 \in \tilde{\mathbf{A}}_2} (x_2 - \mu)^2 &= \sum_{x_2 \in \tilde{\mathbf{A}}_2} ((x_2 - \mu_2)^2 + (\mu_2 - \mu)^2) \\
&= \sum_{x_2 \in \tilde{\mathbf{A}}_2} (x_2 - \mu_2)^2 + (n-k)(\mu_2 - \mu)^2
\end{aligned}$$

Substitute back

$$\begin{aligned}
& nVar(\tilde{\mathbf{A}}) \\
&= \sum_{x_1 \in \mathcal{A}_1} (x_1 - \mu_1)^2 + k(\mu_1 - \mu)^2 + \\
&\quad \sum_{x_2 \in \mathcal{A}_2} (x_2 - \mu_2)^2 + (n - k)(\mu_2 - \mu)^2 \\
&= kVar(\tilde{\mathbf{A}}_1) + (n - k)Var(\tilde{\mathbf{A}}_2) + k(\mu_1 - \mu)^2 + (n - k)(\mu_2 - \mu)^2
\end{aligned}$$

Substituting this into the upper bound, we get

$$\begin{aligned}
\lambda &< \frac{nVar(\tilde{\mathbf{A}}) - (kVar(\tilde{\mathbf{A}}_1) + (n - k)Var(\tilde{\mathbf{A}}_2))}{\frac{n}{k} + \frac{n}{n-k} - 1} \\
&= \frac{k(\mu_1 - \mu)^2 + (n - k)(\mu_2 - \mu)^2}{\frac{n}{k} + \frac{n}{n-k} - 1} \\
&< \max_{1 \leq k < n} \frac{k(\mu_1 - \mu)^2 + (n - k)(\mu_2 - \mu)^2}{\frac{n}{k} + \frac{n}{n-k} - 1}
\end{aligned}$$

We can further simplify the numerator.

$$\begin{aligned}
& k(\mu_1 - \mu)^2 + (n - k)(\mu_2 - \mu)^2 \\
&= k(\mu_1 - \frac{k\mu_1 + (n - k)\mu_2}{n})^2 + (n - k)(\mu_2 - \frac{k\mu_1 + (n - k)\mu_2}{n})^2 \\
&= k(\frac{n\mu_1 - k\mu_1 - (n - k)\mu_2}{n})^2 + (n - k)(\frac{n\mu_2 - k\mu_1 - (n - k)\mu_2}{n})^2 \\
&= k(\frac{(n - k)\mu_1 - (n - k)\mu_2}{n})^2 + (n - k)(\frac{-k\mu_1 + k\mu_2}{n})^2 \\
&= k(\frac{(n - k)(\mu_1 - \mu_2)}{n})^2 + (n - k)(\frac{-k(\mu_1 - \mu_2)}{n})^2 \\
&= \frac{k(n - k)^2(\mu_1 - \mu_2)^2 + (n - k)k^2(\mu_1 - \mu_2)^2}{n^2} \\
&= \frac{kn - k^2 + k^2}{n^2} (n - k)(\mu_1 - \mu_2)^2 \\
&= \frac{k}{n} (n - k)(\mu_1 - \mu_2)^2
\end{aligned}$$

So the upper bound is

$$\lambda < \max_{1 \leq k < n} \frac{\frac{k}{n} (n - k)(\mu_1 - \mu_2)^2}{\frac{n}{k} + \frac{n}{n-k} - 1}$$

Keep in mind we want to balance the efficiency and accuracy, so we don't want to get too close to the precise upper bound, which only considers efficiency; hence, we can estimate the upper bound with a faster calculation. Using $k = \frac{n}{2}$

$$\begin{aligned}
\lambda &< \frac{\frac{\frac{n}{2}}{n} (n - \frac{n}{2})(\mu_1 - \mu_2)^2}{\frac{\frac{n}{2}}{n} + \frac{n - \frac{n}{2}}{n - \frac{n}{2}} - 1} < \max_{1 \leq k < n} \frac{\frac{k}{n} (n - k)(\mu_1 - \mu_2)^2}{\frac{n}{k} + \frac{n}{n-k} - 1} \\
\lambda &< \frac{\frac{1}{2}(\frac{n}{2})(\mu_1 - \mu_2)^2}{2 + \frac{n}{2} - 1} \\
&= \frac{\frac{n}{4}(\mu_1 - \mu_2)^2}{3} \\
&= \frac{n(\mu_1 - \mu_2)^2}{12}
\end{aligned}$$

Finally, we have

$$\lambda_{min} = \frac{(|a_1| - |a_2|)^2}{3n} < \lambda < \frac{n(\mu_1 - \mu_2)^2}{12} = \lambda_{max} \quad (10)$$

And we can control λ through $\tilde{\lambda} \in [0, 1]$ by

$$\begin{aligned}
\lambda &= \lambda_{min} + \tilde{\lambda}(\lambda_{max} - \lambda_{min}) \\
&= \frac{(|a_1| - |a_2|)^2}{3n} + \tilde{\lambda}(\frac{n(\mu_1 - \mu_2)^2}{12} - \frac{(|a_1| - |a_2|)^2}{3n})
\end{aligned}$$

A good λ should be located somewhere in the latter half of the bound, not too close to the upper bound for quantization of LLMs. Notice that a precise λ leads to a specific optimal group size that can be found via binary searching on the result group size from Algorithm 1. Since this is too computationally intensive, we guess $\tilde{\lambda} = 0.75$. Empirical results show λ have indifferent impact on quantization performance.

Appendix C: Experiments and Evaluations

This section presents additional details regarding our experiments and evaluations. By providing granular details, we aim to ensure clarity and transparency, enabling readers to fully understand our experimental framework.

Seven QA tasks. We use seven QA tasks in our study: ARC-C (Abstraction and Reasoning Challenges) and ARC-E (Abstraction and Reasoning Corpus Easy) assess performance in complex/simple reasoning tasks; BoolQ measures accuracy in answering yes/no questions; HellaSwag tests ability in generating coherent text continuations; OPQA (Open-Book Question Answering) accesses performance in open book question answering; PIQA (Physical Interaction QA) evaluates commonsense reasoning in physical interactions; and Winogrande examines context-dependent ambiguity resolution. Avg. (Average Performance) is the average performance across these benchmarks provides a comprehensive overview of the models' capabilities. The higher score in all these benchmarks suggests better model performance.

PPL performance. In LLMs, perplexity (PPL) measures the uncertainty of the model when predicting the next word. A lower perplexity indicates that the model is more confident in its predictions. We compare the PPL of our method against SOTA binary quantification and 4-bit quantification. From Table 6, we can see that our method achieves performance comparable to FP in terms of perplexity, while outperforming the existing SOTA methods for both binary quantization and 4-bit quantization.

Additional experiments setup. Additional experiments are conducted on the proposed algorithms using a randomly generated normal distributed matrix of $\mu = 0$ and $\sigma = 1$, simulating LLMs weights on a single CPU. We compare quantization loss, time, and the impact of different hyperparameter settings in terms of Mean Squared Error (MSE) for both small and large matrices.

Comparison for quantization loss. All three algorithms have their quantization loss in terms of MSE test on a small squared matrix compared with XNOR, Blocked XNOR, and a dummy 0 matrix as shown in Figure 2. In the figures, the dummy has the highest loss for reference, then XNOR and Blocked XNOR have middle MSE and the proposed methods have nearly 0 MSE. It can be noticed at the end of Algorithm 3 (red line), it becomes the same as the XNOR methods, this

Model	Method	Bit len	Wikitext 2	PTB	C4	Avg.
3.2 1B	FP	16	9.75	17.59	14.01	13.78
	GPTQ	4	57.11	81.77	90.41	76.43
	BiLLM	1.08	2119.91	3077.68	1161.44	2119.68
	PB-LLM	1.7	204.28	299.19	235.98	246.48
	WGM	1.007	10.04	18.04	14.45	14.18
	FP	16	7.81	13.53	11.33	10.89
3.2 3B	GPTQ	4	12.23	23.60	15.43	17.09
	BiLLM	1.08	123.09	168.06	100.68	130.61
	PB-LLM	1.7	122.37	149.22	116.41	129.33
	WGM	1.007	8.53	15.24	12.97	12.25
	FP	16	10.51	22.29	19.47	17.42
	Falcon3- GPTQ	4	27.11	63.73	62.39	51.08
1B- 3B- Instruct	BiLLM	1.08	36.74	81.78	68.57	62.36
	PB-LLM	1.7	40.32	121.61	74.09	78.67
	WGM	1.007	10.93	23.50	20.44	18.29
	FP	16	10.11	20.19	18.27	16.19
	Falcon3- GPTQ	4	15.57	42.65	40.17	32.80
	BiLLM	1.08	98.71	274.39	205.57	192.89
Instruct	PB-LLM	1.7	69.19	202.27	148.61	140.02
	WGM	1.007	10.71	21.16	18.84	16.90
	FP	16	434.09	1258.77	478.15	723.67
	GPTQ	4	499.64	1548.70	512.99	853.77
	BiLLM	1.08	2665.29	7618.57	1990.78	4091.54
	PB-LLM	1.7	1490.44	4713.06	1259.44	2487.65
3-1b-it Gemma- 3-4b-it	WGM	1.007	477.50	1431.29	511.50	806.76
	FP	16	81.81	751.01	106.47	313.10
	GPTQ	4	87.45	814.49	106.56	336.16
	BiLLM	1.08	482.59	3857.18	363.00	1567.59
	PB-LLM	1.7	454.86	4608.31	361.43	1808.20
	WGM	1.007	81.74	809.33	109.63	333.57

Table 6: PPL (Perplexity) comparison.

is because the window size is too large and uses n , making it identical to XNOR. This change in window size is caused by the implementation of the test, if the matrix is large enough, it will use a bigger window dynamically. Then in Figure 3, Algorithm 1 is omitted due to infeasible time to completion, and squared matrix of size from 2 to 2048, increasing by the power of 2, is used. As the matrix become bigger, the curve resemble a smoother version of the curve in Figure 2, hinting the generalizability of the smaller matrix test and the approximation accuracy of Algorithm 3 and 2 to the optimal solution from Algorithm 1. A surprise finding in this small matrix test is the MSE loss of all 3 proposed algorithms is all close to 0, despite the MSE of them is rank as hypothesized, Algorithm 1 < Algorithm 2 < Algorithm 3. The error caused by fast approximation in algorithms 2 and 3 is negligible small compared to the theoretically best possible loss from Algorithm 1.

Comparison for quantization speed. With a similar experiments set up in previous section, in this session, MSE is substitute with quantization time and we compare the quantization speed (time used) on both small and large square matrices. As shown in Figure 4, Blocked XNOR and XNOR are the fastest two, then Algorithm 3 (red) and 2 (purple) are the second fastest, and Algorithm 1 (green) is the slowest. This is as expected since Algorithm 1 is the most precise one but has high time complexity, while Algorithm 2 and 3

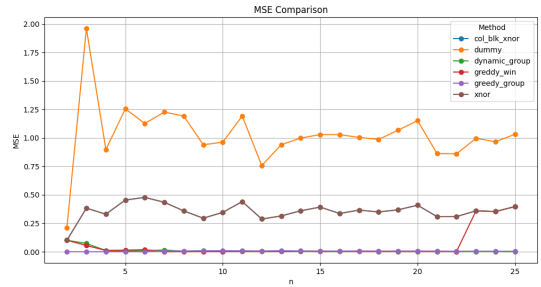


Figure 2: Algorithm comparison for small matrix, quantization loss against matrix sized $\mathbb{R}^{n \times n}$.

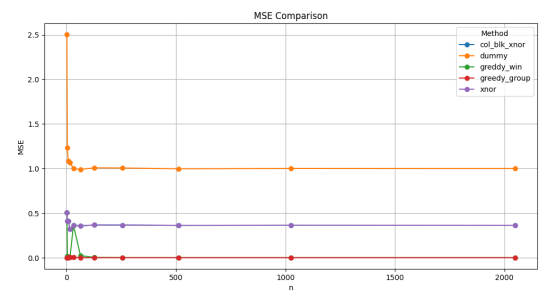


Figure 3: Algorithm comparison for large matrix, quantization loss against matrix sized $\mathbb{R}^{n \times n}$.

have much lower time complexity. Meanwhile, XNOR and block XNOR are the fastest since they only need to compute the mean scalers and sign matrix, and serve as the fastest quantization time reference. Notice the sudden speed up of Algorithm 3 (red) is caused by the same implementation issue in the previous session. As the matrix size increase, the quantization time increase exponentially and Algorithm 1 become infeasible to run to completion, so in Figure 5, we tested quantization on bigger matrix same as the bigger matrix test in the previous session. As the matrix size increases exponentially, Algorithm 2 (red) needs more than 1000 seconds for quantization, while Algorithm 3 (green) only needs less than 10 seconds, 2 order faster than Algorithm 2. Meanwhile XNOR and Blocked XNOR are still the fastest ones but become close to our Algorithm 3 as the size keep increasing. Since Algorithm 3 is the fastest among all three algorithms proposed and the difference of loss of all proposed algorithms is negligible, Algorithm 3 is the most feasible, and will be main methods to be experimented.

Comparison for loss against λ for greedy algorithm and windowed version. Loss of proposed algorithm against different λ also has been experimented in Figure 6. We used matrix $\in \mathbb{R}^{512 \times 512}$ for the experiments to balance computational resources and matrix size. Again only Algorithm 2 and Algorithm 3 are used due to feasibility in actual implementation. As expected, since λ is designed for Algorithm 1 only, both Algorithm 1 and 2 work better when $\lambda = 0$. Also, notice for Algorithm 3 (blue) the variation caused by

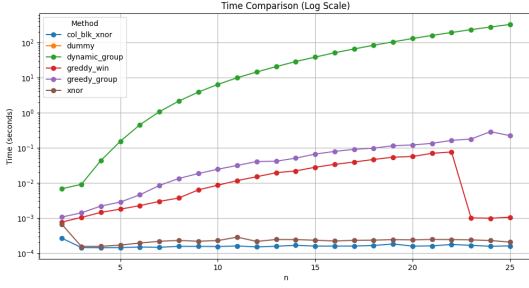


Figure 4: Algorithm comparison for small matrix, time used for quantization on CPU against matrix sized $\mathbb{R}^{n \times n}$.

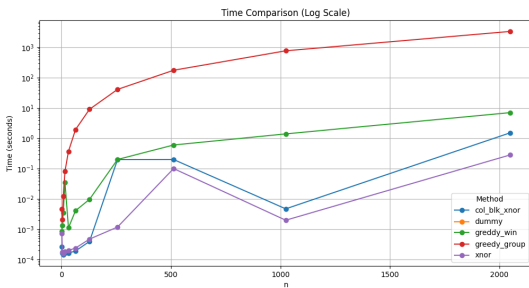


Figure 5: Algorithm comparison for large matrix, time used for quantization on CPU against matrix sized $\mathbb{R}^{n \times n}$.

λ is so small, it is negligible, resemble the QA performance variation of different λ in the main body. This again hinting the accuracy of small matrix test approximating the actual LLMs test. Lastly, since λ is not helping at choosing a good max number of group, we must choose the max number of groups (max group) as a hyperparameter manually.

Comparison for max groups against MSE and speed. Since we need to choose the max group manually, experiments have been conducted on how the max group affects the quantization error and speed on matrix $\in \mathbb{R}^{512 \times 512}$ as in Figure 7 and 8. Notice the point in the figures points increase in power of 2 from left to right, i.e. 2, 4, ..., 131072. We

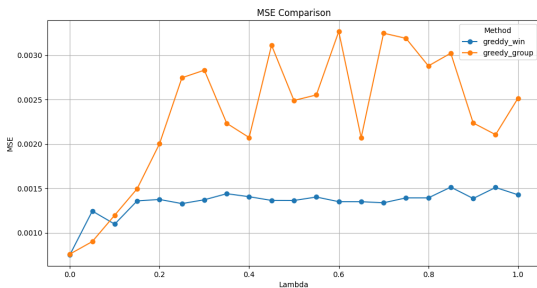


Figure 6: Loss against λ for greedy algorithm and windowed version.

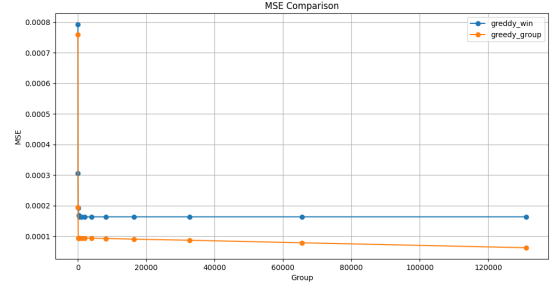


Figure 7: Max groups against MSE.

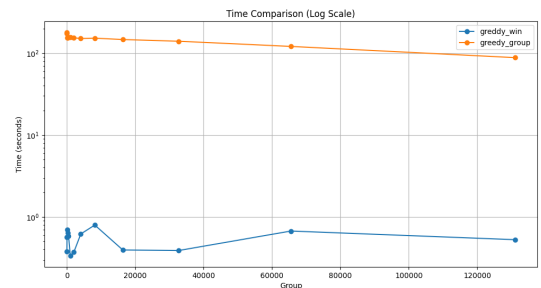


Figure 8: Max groups against quantization speed.

stopped as $131072 = 2^{17}$, since $512^2 = 2^{18}$, further increasing the number of groups will result in the original matrix. From the figures, it can be seen the decrease of MSE of both algorithms 2 (blue) and 3 (orange) flattened out at around 32 max groups. As for the quantization time used, the larger the max group, the faster it is.

Comparison for theoretical average bit length. Notice in Figure 9, that the higher the max group, the longer the average bit length, this is because we need a full precision scaler for each group, so the ratio of 16 bits number to 1-bit number also increase and give longer average bit length.

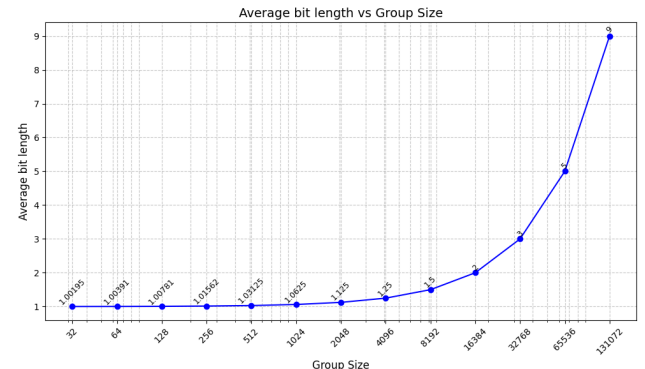


Figure 9: Theoretical average bit length.

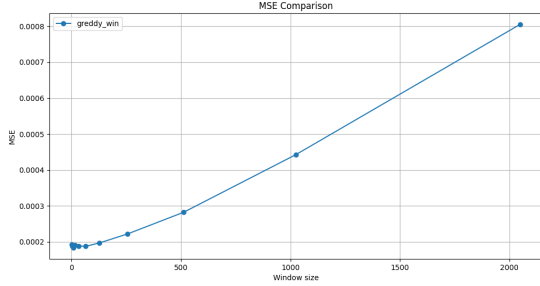


Figure 10: Window (initial group) size against loss.

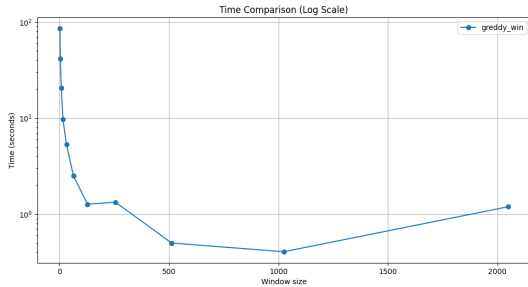


Figure 11: Window (initial group) size against quantization speed.

Comparison for window (initial group) size against quantization loss and speed. Lastly, for matrix simulation experiments, the impact of different window sizes for Algorithm 3 on MSE and quantization speed has also been tested as in Figure 10 and 11. It has shown that as the window size increases the MSE increases and the quantization time decreases. Notice when the Window size is below 64, the MSE is about the minimum, and as the window size increases 64 to 1024, the quantization time decreases flattened out. Thus, to balance the quantization performance and speed, window size 64 is used.

Throughout the matrix simulation experiments, the results and conclusions drawn closely resemble the results and conclusions drawn from QA performance on LLMs quantized using the same algorithm. This suggests that the quantization performance of LLMs can be reflected by the performance of full weights to a certain degree. However, the detailed causal relationship is outside the scope of this research and is therefore omitted.